Available online at www.sciencedirect.com

ScienceDirect

Mendeleev Commun., 2022, **32**, 837–839

Mendeleev Communications

IR spectroscopic study of the hydrogen bond network in the water–3-amino-1-propanol system and its comparison with the spatial network of hydrogen bonds in the water–monoethanolamine system

Elena G. Kononova,[a] Irina A. Solonina,[b] Margarita N. Rodnikova*[b] and Ekaterina V. Shirokova[b]

[a] *A. N. Nesmeyanov Institute of Organoelement Compounds, Russian Academy of Sciences, 119991 Moscow, Russian Federation. E-mail: lena.kononova@gmail.com*

[b] *N. S. Kurnakov Institute of General and Inorganic Chemistry, Russian Academy of Sciences, 119991 Moscow, Russian Federation. E-mail: rodnikova@igic.ras.ru*

DOI: 10.1016/j.mencom.2022.11.043

IR spectroscopy was used to explore the water–3-amino-1-propanol (3AP) system in the range of 400–4000 cm^{-1}. Based on the stretching vibrations of OH, NH_2 and CH groups and skeletal bending vibrations of 3AP it was concluded that mixed spatial networks are formed in the water–3AP system that predominate at medium 3AP concentrations. The obtained results are similar to the IR spectroscopic data for the water–monoethanolamine system, *viz.*, the networks of both amino alcohols are incorporated into the spatial network of water to form mixed hydrogen bond networks.

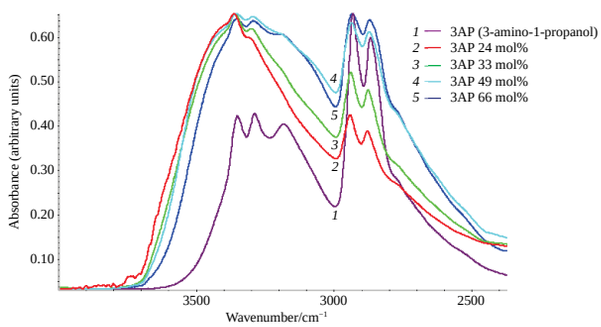

Keywords: liquid amino alcohols, water–amino alcohol systems, hydrogen bond networks, IR spectroscopy.

Similarly to water, liquid amino alcohols have a spatial network of hydrogen bonds that shows stability, lability and elasticity, along with adjustment of the various motion types of the molecules that form the network.[1] Aqueous solutions of amino alcohols form mixed networks of H-bonds, their structure depending on the concentration, temperature, and nature of amino alcohols.[2] We explored the aqueous system of aliphatic amino alcohol, namely 3-amino-1-propanol (3AP), and compared it with the aqueous system of monoethanolamine (MEA).[3] Both systems are very important in cryobiology.[4–10] The water–3AP system manifesting high supercooling of the liquid phase has been recently used for the long-term storage of living cells and organs.[11,12] The high supercooling is caused by the stability of the spatial network of hydrogen bonds in aqueous solutions of amino alcohols.[1] The molecular structures of these amino alcohols in the gas phase obtained by the quantum-chemical calculations are shown in Figure 1. The molecules in the gas and liquid phase have the preferred *gauche* conformation.[13–15]

The rigidity of MEA molecules compared with 3AP should be noted, as well as the increased flexibility of 3AP molecules and higher energy of the intramolecular H-bond in 3AP molecules compared with MEA due to the presence of a $(CH_2)_3$ bridge in 3AP.[11] The physicochemical properties of 3AP, MEA and H_2O are presented in Online Supplementary Materials (Table S1). It can be concluded from the data that the H-bonds network in 3AP is somewhat more stable than in MEA as displayed by the lower compressibility β_T value of 3AP.

We have used mathematical methods to describe the mixed networks of hydrogen bonds in the water–MEA system: molecular dynamics, graph theory and Delaunay simplexes,[2] along with IR spectroscopy for confirmation.[3] The results allow us to conclude that at low MEA concentrations, its spatial network of H-bonds is incorporated into the water network, while, in contrast, at high concentrations the network of water H-bonds is incorporated into the network of 3AP H-bonds. Of particular interest are medium concentrations. Mixed networks predominate at these concentrations, as shown by calculations and confirmed by the mixing enthalpy, and it is mixed networks that exist in the liquid phase at low temperatures.[2]

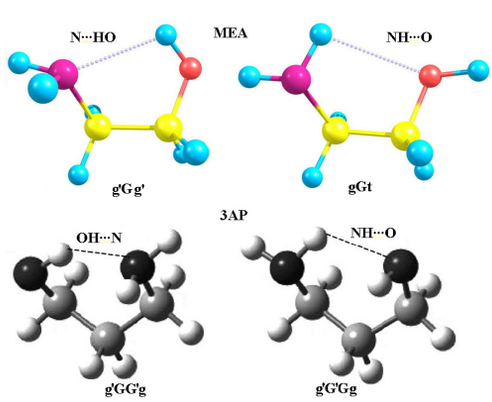

Figure 1 Calculated molecular structures of MEA and 3AP.

We used IR spectroscopy to describe the H-bonds network in the water–3AP system and compared it to the H-bonds network in the water–MEA system.† The spectrum of pure 3AP in the

† IR spectra of the liquids were recorded in the region of 4000–400 cm^{-1} on a Bruker Tensor 37 Fourier IR spectrometer in thin layer between KBr and CaF_2 windows.

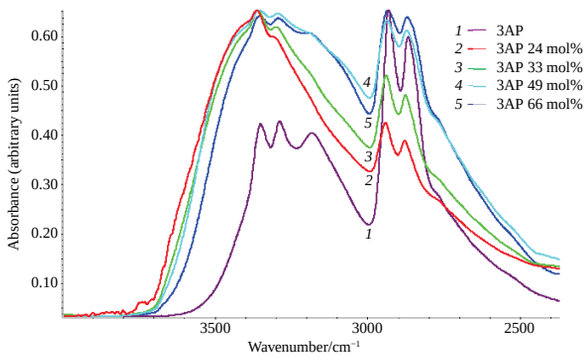

Figure 2 IR spectra of water–3AP mixtures in the region of 4000–2400 cm^{-1}.

range of 4000–2400 cm^{-1} (Figure 2), the region of OH, NH_2 and CH stretching vibrations, is very similar to the MEA spectrum and has a few intense overlapping bands at 3350 cm^{-1} [$\nu_{as}(NH_2)$], 3290 cm^{-1} [$\nu_s(NH_2)$], 3182 cm^{-1} [ν(intermolecular H-bonds)], 2931 and 2866 cm^{-1} [ν(CH)].

In water–3AP mixtures containing not less than 66 mol% of water, the band of intermolecular H-bonds in 3AP (3182 cm^{-1}) almost disappears, which indicates their cleavage. At the same time, the low-frequency wing of this combined band is shifted by *ca*. 100 cm^{-1} towards the low frequencies with respect to 3AP and by *ca*. 500 cm^{-1} with respect to water, which indicates that a mixed network of hydrogen bonds between 3AP and water is formed.

The lineshape narrowing of the bands observed in the 4000–2400 cm^{-1} range upon transition from 49 mol% through 33 mol% to 24 mol% of 3AP indicates the spatial H-bond network simplification. The total match between the absorption bands of pure water and its mixture with 24 mol% 3AP in the high-frequency region suggests the water phase existence at this 3AP content. At the same time, the low-frequency wing of this combined band of the water–3AP mixture is noticeably shifted to the low-frequency region with respect to the band of pure water. This also indicates the presence of a mixed water–3AP network having volume which decreases noticeably with a decrease in molar fraction of 3AP in the system, based on the character of spectral changes depending on the mixture composition (the absorption bands of OH- and NH-groups in the low-frequency region become narrower with a decrease in the 3AP fraction).

The data obtained for the water–3AP system compared with the similar data for the water–MEA system shows that the mixed network of H-bonds of the water–3AP mixture is characterized by stronger H-bonds, since the maximum of the ν(OH, NH) band (3200 cm^{-1}) is shifted by 150 cm^{-1} towards lower frequencies compared to that of the water–MEA system (3350 cm^{-1}).

A particularly significant difference between water–MEA and water–3AP systems is noted for the half-width of the ν(OH, NH) band. For example, its value is 600 cm^{-1} in the case of water–MEA and 800 cm^{-1} in the case of water–3AP when the

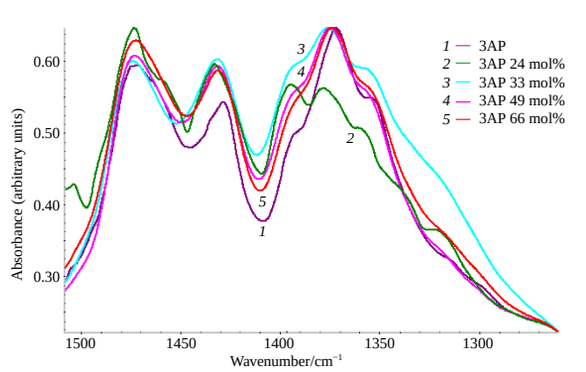

Figure 3 IR spectra of water–3AP mixtures in the region of 1550–1200 cm^{-1}.

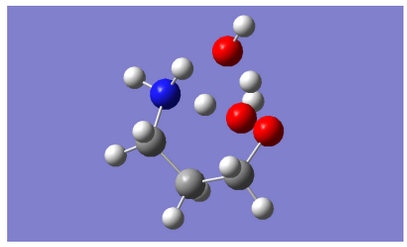

Figure 4 Optimized geometry of 3AP·$2H_2O$ [B3LYP 6-311++G(d,p)].

fraction of amino alcohol in the mixture is ~50 mol%. This indicates a more complex (more differentiated) structure of the mixed network of H-bonds in the water–3AP system.

In the region of C–O skeletal vibrations in 3AP (1075–1040 cm^{-1}) no significant changes were observed upon an increase in water content in the water–3AP system, which can be explained by an insignificant effect of interaction with water on the force constants of C–O bonds in 3AP molecules.

However, the dependence of the intensities of the three bands of skeleton bending vibrations in the region of 1550–1200 cm^{-1} (Figure 3) on the system composition was observed. In pure 3AP, the band at 1370 cm^{-1} is the most intense among these three bands (1340, 1370 and 1390 cm^{-1}). At 24 mol% of 3AP, the band at 1390 cm^{-1} becomes the most intense, and a noticeable change in the ratios of the intensities of the above bands occurs as the 3AP fraction decreases below 33 mol%. This spectral behavior indicates that the conformation of 3AP molecules depends on the molar composition.

This assumption agrees with the data of quantum-chemical calculations [B3LYP 6-311++G(d,p)] for the 2:1 water:3AP system. According to the calculations, the formation of H-bonds between one 3AP molecule and two water molecules results in a change in the 3AP geometry from *gauche*- to *cis*-form (Figure 4) which, according to the IR data, may become dominant in the solution.

Thus, according to IR spectroscopy data, the H-bond network of 3AP in the water–3AP system with the 2:1 ratio of H_2O:3AP components is broken and a mixed network of water–3AP hydrogen bonds is formed.

As the fraction of 3AP in the system decreases below 33 mol%, the content of the initial 3AP conformer decreases markedly due to its transition to the *cis*-form, as quantum-chemical calculations predict.

The results obtained in this work compared with those obtained previously by IR spectroscopy of the water–MEA system show a great similarity with the water–3AP system: in both cases mixed water–amino alcohol networks are formed that predominate in the region of average amino alcohol concentrations. However, in the case of the water–3AP system, stronger H-bonds are formed along with a less ordered mixed network, which may be explained by the greater flexibility of the 3AP skeleton and its ability to adopt spatial arrangements that are more diverse and energetically more favorable for the formation of H-bonds.

This work was financially supported by the Ministry of Science and Higher Education of the Russian Federation as a part of the state assignment to the N. S. Kurnakov Institute of General and Inorganic Chemistry of the Russian Academy of Sciences and as a part of the state assignment to the A. N. Nesmeyanov Institute of Organoelement Compounds of the Russian Academy of Sciences.

Online Supplementary Materials

Supplementary data associated with this article can be found in the online version at doi: 10.1016/j.mencom.2022.11.043.

References

1 M. N. Rodnikova, *Russ. J. Phys. Chem.*, 1993, **67**, 248 (*Zh. Fiz. Khim.*, 1993, **67**, 275).
2 M. N. Rodnikova, G. M. Agayan, N. K. Balabaev, I. A. Solonina and E. V. Shirokova, *Russ. J. Phys. Chem. A*, 2021, **95**, 974 (*Zh. Fiz. Khim.*, 2021, **95**, 770).
3 E. G. Kononova, M. N. Rodnikova, I. A. Solonina and E. V. Shirokova, *RENSIT*, 2021, **13**, 169.
4 Yu. P. Klapshin, I. A. Solonina, M. N. Rodnikova, M. R. Kiselev, A. V. Khoroshilov and S. V. Makaev, *Mendeleev Commun.*, 2020, **30**, 534.
5 J. S. Clegg, *Comp. Biochem. Physiol., Part B: Biochem. Mol. Biol.*, 2001, **128**, 613.
6 E. Shalaev and F. Franks, in *Amorphous Food and Pharmaceutical Systems*, ed. H. Levine, RSC Publishing, Cambridge, UK, 2002, pp. 200–215.
7 M. P. Buera, Y. Roos, H. Levine, L. Slade, H. R. Corti, D. S. Reid, T. Auffret and C. A. Angell, *Pure Appl. Chem.*, 2011, **83**, 1567.
8 L. Slade, H. Levine and D. S. Reid, *Crit. Rev. Food Sci. Nutr.*, 1991, **30**, 115.
9 P. M. Mehl, *Thermochim. Acta*, 1993, **226**, 325.
10 V. I. Grischenko, *Probl. Cryobiol.*, 2005, **15**, 231 (*Probl. Kriobiol.*, 2005, **15**, 231).
11 A. Baudot, C. Cacela, M. L. Duarte and R. Fausto, *Cryobiology*, 2002, **44**, 150.
12 L. Luo, Y. Pang, Q. Chen and G. Li, *CryoLetters*, 2006, **27**, 341.
13 Yu. V. Novakovskaya and M. N. Rodnikova, *Russ. J. Inorg. Chem.*, 2014, **59**, 1290 (*Zh. Neorg. Khim.*, 2014, **59**, 1534).
14 D. L. Thomsen, J. L. Axson, S. D. Schrøder, J. R. Lane, V. Vaida and H. G. Kjaergaard, *J. Phys. Chem. A*, 2013, **117**, 10260.
15 S. M. Melnikov and M. Stein, *J. Phys. Chem. B*, 2018, **122**, 2769.

Received: 16th May 2022; Com. 22/6896